

## **Numerical simulation of two-phase separation in T-junction with experimental validation**

**Minh Tran, Zeeshan Memon, Ahmed Saieed, William Pao\* and Fakhrudin Hashim**

Faculty of Mechanical Engineering, Universiti Teknologi PETRONAS  
32610 Seri Iskandar, Perak, Malaysia,  
\*Email: [william.pao@utp.edu.my](mailto:william.pao@utp.edu.my)

### **ABSTRACT**

Liquid carryover in T-junction due to splitting nature of two-phase flow causes serious issues for downstream equipment which is not designed to handle excessive liquid. In this paper, the phenomena of liquid carryover in T-junctions were analyzed using the Volume of Fraction (VOF) together with the  $k-\varepsilon$  turbulence model. T-junction separation efficiency was measured through mass flow rate fraction of air and water between the branch and main arm over a range of diameter ratios 0.6 to 1.0, water superficial velocity 0.186 to 0.558 m/s and air superficial velocity 4 to 8 m/s. The results showed simulation model was successfully validated with average deviation of less than 5% and can be used to predict phase split of slug flow in T-junction. The numerical model confirmed the significant influence of diameter ratio and superficial velocities of air and water on phase split. Reduced T-junction delivers better separation performance compared to regular T-junction. In slug flow regime, T-junction's performance can be improved by either decreasing air velocity or increasing water velocity. A new dimensionless parameter, namely the area under the curve of separation efficiency (S), was proposed and proved as a qualified judging criteria for evaluating phase separation efficiency of T-junctions.

**Keywords:** Two-phase separation; T-junction; numerical simulation; slug flow.

### **INTRODUCTION**

An original branching T-junction consists the straight main pipe joined perpendicularly at the intersection by a branch arm as shown in Figure 1 [1]. In the oil and gas industry, T-junctions are used widely for many purposes, one of which is the partial two-phase separator based on the principle of inertia difference between the two phases. Instead of using fully-equipped separators, T-junction is preferred for preliminary separation of well fluids accumulated at production headers. T-junction shows some economical and technical advantages such as much cheaper capital and operating cost and space saving in offshore platform. The separated gas from these processes is fed into gas intensive treatment system to produce instrument gas, gas lift and injection gas, which require a much higher level of dryness. Therefore, excessive liquid carryover in gas feed causes serious issues for downstream instruments, even trips the entire system. Multiphase separation at the T-junction is detected as the root cause for liquid carryover problem. Thus, many research work has been conducted to improve T-junction separation efficiency.

In-depth literature survey reveals that flow regime is one of the most dominant factors in phase split results [2–5]. Depending on many parameters such as pipe diameter, phase properties and inlet relative superficial velocities, different flow regime can appear in the pipe [4, 6]. On the other hand, previous works mostly focus on the separation efficiency of T-junctions taking into account the effect of geometry, orientation and fluid properties but the impact of flow regime evolution on its separation was not discussed in all aspects. In case of slug flow, although it is very common in practice, few investigations have been devoted to address its separation behavior due to its nature of complexity. Thus, more attempts should be spent on investigating the phase split of slug flow.

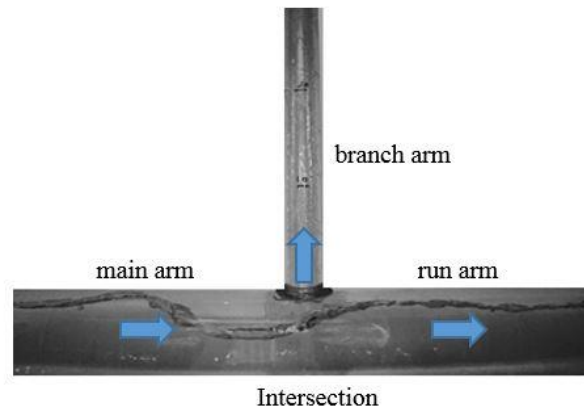


Figure 1. Air-water flow in a branching T-junction

Overall, investigation methodology on two-phase separation can be divided into three main methods, namely experiment, analytical solution and computational fluid dynamics (CFD) simulation [7, 8]. Together with a rapidly growing capacity of computation, CFD is attractive to not only the industry but also academic research since it is more cost-effective than physical-testing and allows detailed investigation in the complicated flow. Simulation, therefore, plays an important role and valuable tool for study [9]. Among many methods in CFD, Volume of Fraction (VOF) is a proven tool of tracking interface to be used as a preference in studying intermittent flow in straight pipes such as bubbly flow [10–12], slug flow [13–17]. However, relatively few simulations on slug flow in T-junction have been published. Therefore, this paper employs VOF to extend prior numerical study of slug flow over T-junction. Validated model can be used to study slug flow in T-junction in detail and predict its phase split to improve its separation efficiency using new proposed criteria. The effects of diameter ratio and superficial velocities of air and water on phase split efficiency are described and discussed. The results are expected to promote the advantages of VOF methods in the study of two-phase flow in T-junction.

## METHODOLOGY

### Geometry Domain and Meshing

Geometry domain of T-junction was taken from Saieed et al [18] which were conducted an experiment for air-water flow loop as shown in Figure 2. Geometry in the present model included the mixer and T-junction. Figure 3 presents a three-dimensional model of T-junction with main, run and branch arms.

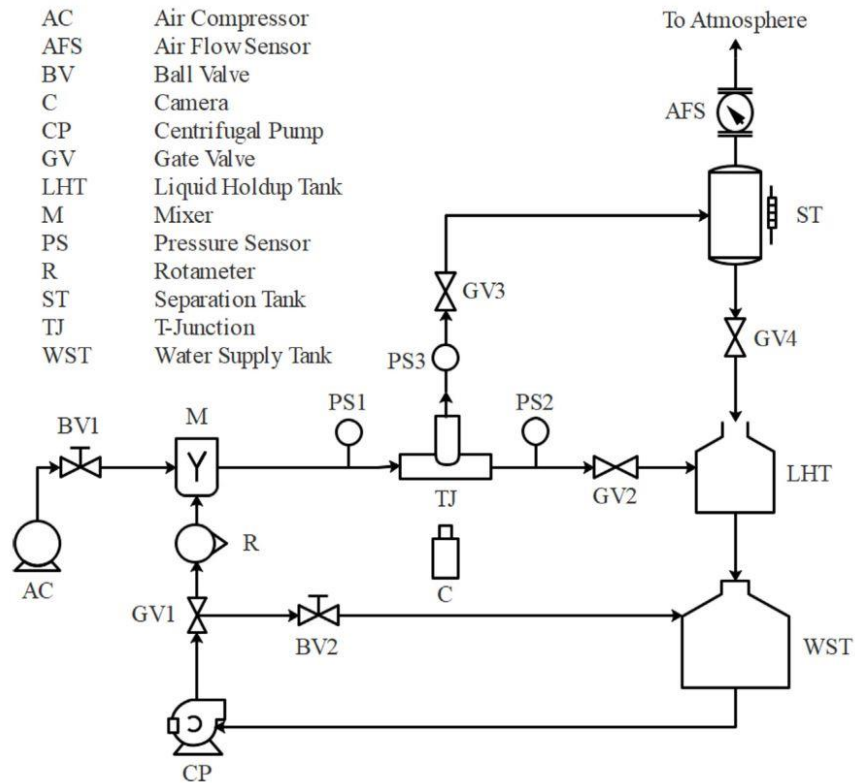


Figure 2. Schematic of the air-water flow loop.

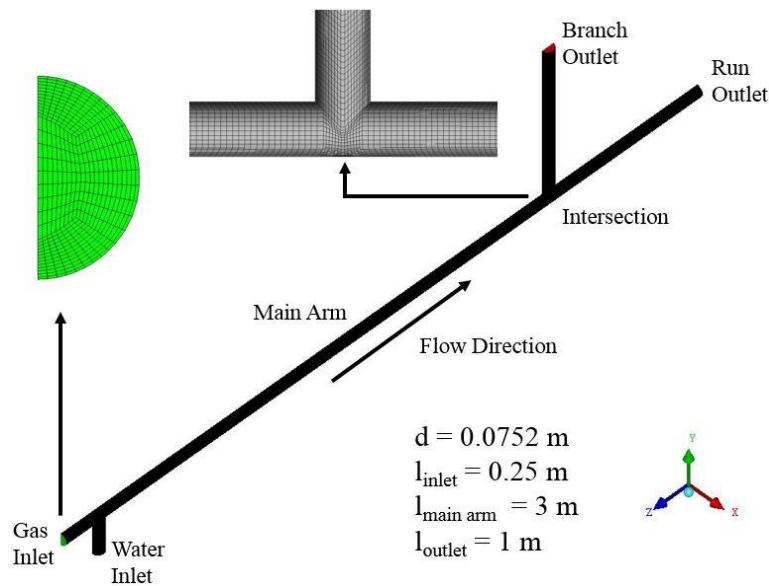


Figure 3. Schematic of the modeling geometry domain with meshing.

To validate the numerical model with experimental data, the ratio of the mass flow rate at branch arm and main arm, namely fraction of air ( $F_a$ ) and water ( $F_w$ ) going to branch arm, is used as indicators of phase distribution as shown in Eq. (1), (2). Meanwhile, the mass flow rate ratio ( $F$ ) is also expressed as Eq. (3).

$$F_a = \frac{m_{a3}}{m_{a1}} \quad (1)$$

$$F_w = \frac{m_{w3}}{m_{w1}} \tag{2}$$

$$F = \frac{m_3}{m_1} \tag{3}$$

where the mass flow rate of air ( $m_a$ ) and water ( $m_w$ ) is calculated as Eq. (4), (5).

$$m_a = \rho_a v_{sa} A \tag{4}$$

$$m_w = \rho_w v_{sw} A \tag{5}$$

Table 1 shows the base case setup for validation and also a range of variables in a further investigation. Apart from 1.0 diameter ratio, 0.6 was chosen because it gives highest air fraction in the side arm [19]. Wall boundary conditions were set to be smooth (no-slip condition), which means velocity at the wall has zero tangential component. In addition, velocity inlet was specified along with the inlet face with the magnitude of velocities shown in Table 2. At the outlet face, static pressure was set as atmospheric pressure (zero-gauge pressure). At outflow boundary condition, no flow properties are specified, instead, normal gradients to the outflow plane of flow properties, for instance, velocity and turbulence quantities, were set to be zero ( $dv/dz = 0$  at the run outlet and  $dv/dy = 0$  at branch outlet). Mass flow split was set to be 0.2, 0.4, 0.5, 0.6 and 0.8. The symmetry boundary condition enabled to model a half of physical geometry domain, thereby saving computational time. Mathematically, normal gradients to the symmetry plane of flow field variables were set to zero throughout the symmetry plane. Gravitational acceleration ( $g = 9.81 \text{ ms}^{-2}$ ) was applied in the reversed y-direction.

Table 1. Base case and parameters' range.

Variables	Unit	Base case	Range
Diameter ratio, $DR$	-	1.0	0.6, 1.0
Air superficial velocity, $v_{sa}$	$\text{ms}^{-1}$	4	4, 8
Water superficial velocity, $v_{sw}$	$\text{ms}^{-1}$	0.186	0.186, 0.31, 0.434, 0.558
Mass flow split	-	0.2	0.2, 0.4, 0.5, 0.6, 0.8

Table 2. Five combinations of superficial velocities of air and water used for validation.

Case	$v_a$ (m/s)	$v_w$ (m/s)	$VR$	$DR$	$G/\lambda$ ( $\text{kg/m}^2\text{s}$ )	$L\lambda\psi/G$ (-)	Flow Regime	Validation Experimental Data
1	4	0.186	21.5	1	4.9	37.9	Slug flow	Wren [3], Saieed [1]
2	4	0.31	12.9	1	4.9	63.2	Slug flow	Wren [3], Saieed [1]
3	4	0.434	9.2	1	4.9	88.4	Slug flow	Wren [3], Saieed [1]
4	4	0.558	7.16	1	4.9	113.7	Slug flow	Wren [3], Saieed [1]
5	8	0.31	25.8	1	9.8	31.6	Slug flow	Wren [3], Saieed [1]
6	4	0.434	9.2	0.6	4.9	88.4	Slug flow	Wren [3]

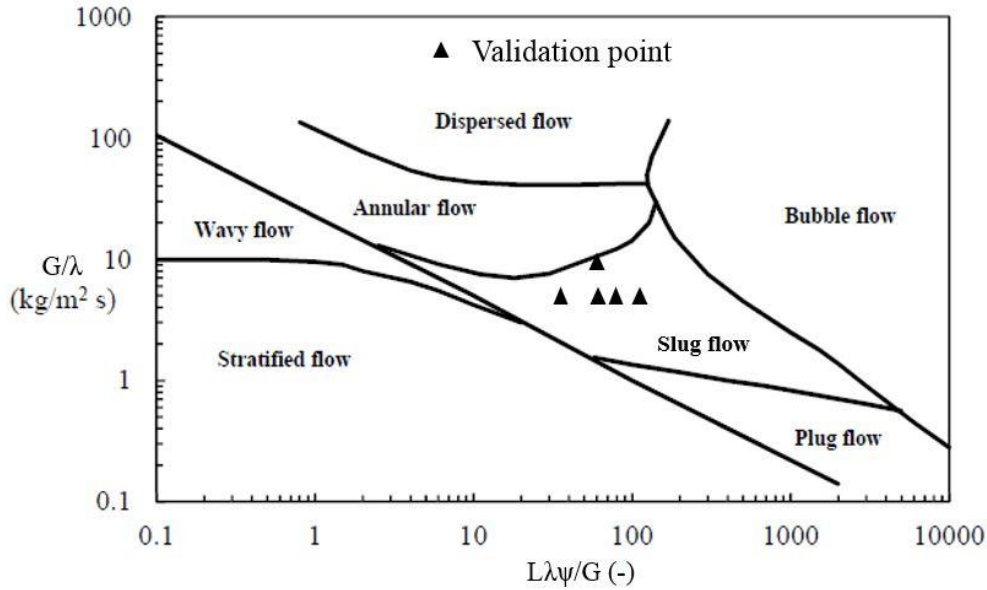


Figure 4: Validation points in Baker chart.

For validation purpose, Table 2 represents six combinations of superficial air and water velocity to generate slug flow based on experimental data from Wren [3], which were presented in Figure 4 [20]. In Wren's work, comprehensive experiments were conducted to evaluate the impact of geometry features on the separation efficiency of T-junction. The diameter ratio varied from 0.6 to 1.0 and he came to conclude that reduced T-junction performs better than regular T-junction in term of reducing liquid-carryover. Moreover, Saieed's experimental data [1] was used to compare with simulation's results. Due to the limited capacity of his experiment, he argued that lower velocity combination of air and water can be used to compare with Wren's data as long as the velocity ratio ( $VR$ ) between air and water shown in Eq. (6) was kept the same. As a result, this work was also validated with Saieed's data. The inlet temperature and pressure were set at constant values of 25°C and 101325 Pa, respectively. Therefore, densities of air and water can be set as 1.225 and 998.2 kg/m<sup>3</sup>. Mass flux of air and water was calculated by Eq. (7), (8).  $\lambda$  and  $\psi$  are dimensionless parameters which equal to 1 in case of air and water. Originally,  $\lambda$  and  $\psi$  were introduced to apply for different working fluids and pipe diameters as shown in Eq. (9), (10).

$$VR = \frac{v_a}{v_w} \quad (6)$$

$$G = v_{sa} \rho_a \quad (7)$$

$$L = v_{sw} \rho_w \quad (8)$$

$$\lambda = \left( \frac{\rho_g \rho_l}{\rho_a \rho_w} \right)^{1/2} \quad (9)$$

$$\psi = \left( \frac{\sigma_w}{\sigma} \right) \left[ \left( \frac{\mu_l}{\mu_w} \right) \left( \frac{\rho_w}{\rho_l} \right)^2 \right]^{1/3} \quad (10)$$

### Governing Equations

According to the previous simulation works on pipes with different flow regime, Eulerian-Eulerian and Volume of Fraction (VOF) modeling are the most popular approaches. Depending on the flow regimes, the first approach is preferred in case of generating bubbly while the latter one is favored in studying the interface between two phases, especially in transition or separation zone. Using a piecewise linear interface calculation (PLIC), VOF approach is described in this work of slug flow.

In the VOF modeling, the phases share a single set of conservation equations. To simulate slug flow with intensive turbulence, the realizable two-equation  $k-\varepsilon$  model is utilized to account for the mixture turbulence considering its flexibility in various situations due to its advantages compared with standard  $k-\varepsilon$  model [21]. The  $k-\varepsilon$  model has been used widely in previous simulation research and proved their sufficient ability to model the two-phase flow in T-junction without expensive computing capacity. This is explained by the fact that, the flow regime evolution and phase separation behavior is dominated by gravitational force and inertia, thus very high resolution in boundary layers and using low-Reynold turbulence model are not necessary. Even though the  $k-\omega$  is also a good candidate to predict reasonably the flow characteristics qualitatively and quantitatively, the computation cost is too high [22]. Therefore,  $k-\varepsilon$  model is employed together with realizable wall treatment. Generally, the governing equations can be written as Eq. (11) - (14).

- Mass conservation equation:

$$\frac{\partial}{\partial t}(\alpha_i \rho_i) + \nabla \cdot (\alpha_i \rho_i v_i) = 0 \quad (11)$$

- Momentum conservation equation:

$$\frac{\partial}{\partial t}(\alpha_i \rho_i v_i) + \nabla \cdot (\alpha_i \rho_i v_i v_i) = -\alpha_i \nabla P + \nabla \tau + \alpha_i \rho_i g + R_{l,g} \quad (12)$$

- Turbulence equation:

$$\frac{\partial(\rho_m k)}{\partial t} + \nabla \cdot (\rho_m k v_m) = \nabla \cdot \left( \frac{\mu_{t,m}}{\sigma_k} \nabla k \right) + G_{k,m} - \rho_m \varepsilon \quad (13)$$

$$\frac{\partial(\rho_m \varepsilon)}{\partial t} + \nabla \cdot (\rho_m \varepsilon v_m) = \nabla \cdot \left( \frac{\mu_{t,m}}{\sigma_\varepsilon} \nabla \varepsilon \right) + \frac{\varepsilon}{k} (C_{1\varepsilon} G_{k,m} - C_{2\varepsilon} \rho_m \varepsilon) \quad (14)$$

where  $\sigma_k$ ,  $\sigma_\varepsilon$ ,  $C_{1\varepsilon}$ ,  $C_{2\varepsilon}$  are 1.0, 1.3, 1.44, 1.92 respectively and the mixture density, velocity, and turbulent viscosity are expressed as Eq. (15) - (17).

$$\rho_m = \alpha_l \rho_l + \alpha_g \rho_g \quad (15)$$

$$v_m = \frac{\alpha_l \rho_l v_l + \alpha_g \rho_g v_g}{\alpha_l \rho_l + \alpha_g \rho_g} \quad (16)$$

$$\mu_{t,m} = C_\mu \rho_m \frac{k^2}{\varepsilon} \quad (17)$$

### Model Verification with Mesh Convergence Analysis

The hexahedral mesh shown in Figure 3 was generated by ICEM CFD using the O-grid method. Ten layers were created in the boundary to capture near-wall flow behaviors. Before doing validation, a mesh independence test was carried out to estimate the optimum mesh size with accurate results. Five cases with different mesh resolution were generated from very coarse to very fine mesh. Then all mesh cases were imported into the same base model as shown in Table 1. Average air fraction at the branch outlet plane

and the pressure drop between section plane A and B was measured to determine the accuracy of the simulation. It is noted that plane A is on the main arm and 1m from the intersection (equivalent to 13d), while plane B is run outlet face. Figure 4 presents that from medium case to the finer resolution, the observed parameters do not change appreciably, and so the medium grid of 357762 cells is adequately resolved and chosen for further investigation.

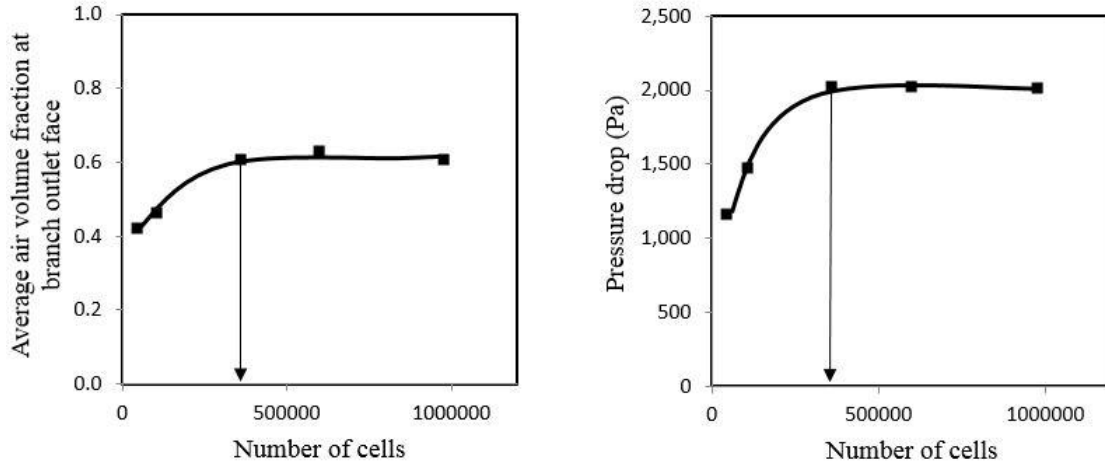


Figure 4. Mesh independence test with 5 different mesh resolution.

## RESULTS AND DISCUSSION

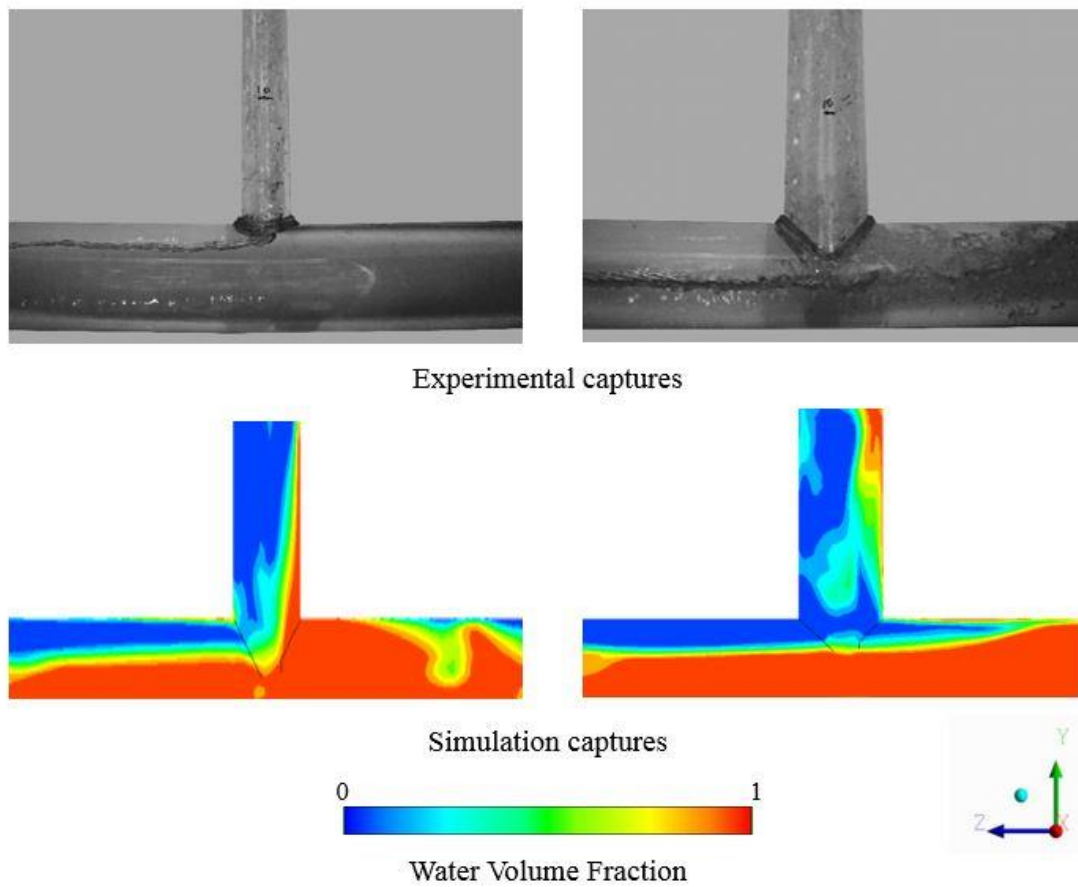
### Model Validation with Experimental Data

Figure 5 compared the contours of water volume fraction with experimental captures of split behavior in T-junction. When the air slug reaches the intersection, an amount of air is directed to the branch arm, which increases the pressure drop between the branch arm and main arm. This leads to the slug jump phenomenon shown in Figure 5a, in which the liquid is dragged into the branch arm. If the dragged force cannot overcome the gravitational force, the slug jump falls back to the main arm as shown in Figure 5b. Verified model was validated with experimental data of Wren [3] and Saieed [1]. The model was set up for a base case with a range of five combinations of air and water velocities shown in Table 2. Simulation result was validated with experimental data using air and water fraction at outlet face of branch arm. Figure 6 presents six figures corresponding to six validation combinations. Simulation data were linearly interpolated to calculate error with experimental data points.

The standard error of the estimate (*SEE*) calculated as Eq. (18) was used to determine the error of predicted simulation results compared to experiment.

$$SEE = \sqrt{\sum \frac{(y - y_{est})^2}{n}} \quad (18)$$

where  $y$  is the experiment data,  $y_{est}$  is the simulation results,  $n$  is number of given data



a) Slug reaching the intersection in reduced T-junction

b) Slug in branch arm falling back in regular T-junction

Figure 5. Model's contours compared with experiment's captures.

Table 3 tabulated the Standard Error of Estimate (*SEE*) of present simulation results with experimental data. The averaged *SEE* relative to Wren's [3] and Saieed's [1] data is 5.29 % and 4.43 %, respectively, which are acceptable for the flow split prediction. Therefore, the model can be used for further investigation.

Table 3. The Standard Error of Estimate (*SEE*) with experimental data

	Case 1	Case 2	Case 3	Case 4	Case 5	Case 6	Average
<i>SEE</i> with Wren [3]	0.0458	0.0254	0.0637	0.0697	0.0734	0.0314	0.0529
<i>SEE</i> with Saieed [1]	0.0335	0.0381	0.0234	0.0229	0.1037		0.0443

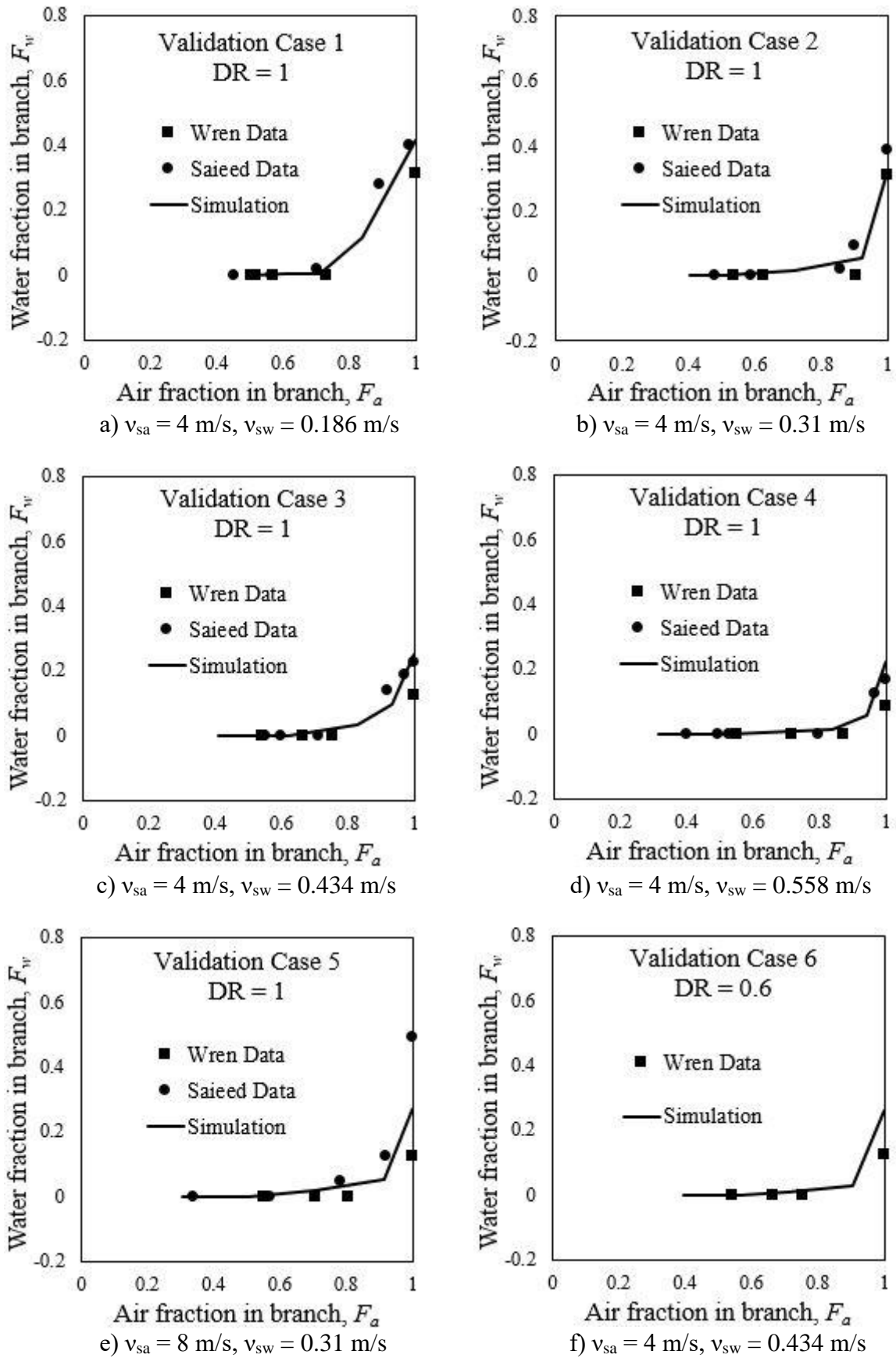


Figure 6. Model validation with experimental data from Wren [3] and Saieed [1].

**Dimensionless Area under the Separation Efficiency Curve**

Previous research on T-junction used Liquid Carryover Threshold (*LCT*) and Peak Liquid Carryover (*PLC*) as a criterion to assess split efficiency [18, 23, 24]. Using Figure 7 as an illustration, *LCT* is the liquid carryover’s onset, in which average water volume fraction at branch outlet surface is nonzero ( $F_w > 0$ ). Meanwhile, *PLC* is the maximum water fraction extracted into branch arm ( $F_a = 1$ ). According to [4, 25], high air fraction at branch caused a high-pressure drop between main and sidearm was blamed to be one of the main reasons for liquid carryover phenomenon. Therefore, *PLC* is normally recorded at the peak of air fraction at the branch. Based on the definition of these two parameters, an optimum T-junction should have high *LCT* but low *PLC* [24]. However, the authors found the severe limitation of using these criteria to judge if a particular T-junction is good for separation. As an example, Figure 7 showed the first T-junction with  $LCT_1$  and  $PLC_1$  and a second T-junction with  $LCT_2$  and  $PLC_2$ . It is obvious that the definition given in [25] as a judging criterion for optimum T-junction resulted in some confusion and ambiguity of choice in this case.

To overcome this ambiguity, these authors proposed to use dimensionless area, *S*, under the curve of separation efficiency as a single-valued scalar indicator to evaluate a T-junction’s performance. *S* is a dimensionless parameter defined as the area of the region bounded by the axis and linear interpolated curve from a set of data of air and water fraction. The area under the curve can be calculated using standard numerical integration formula, e.g. trapezoidal rule. Figure 7 illustrates  $S_1$  of T-junction 1 and  $S_2$  of T-junction 2, respectively. From common sense, optimum T-junction should have a minimum *S*.

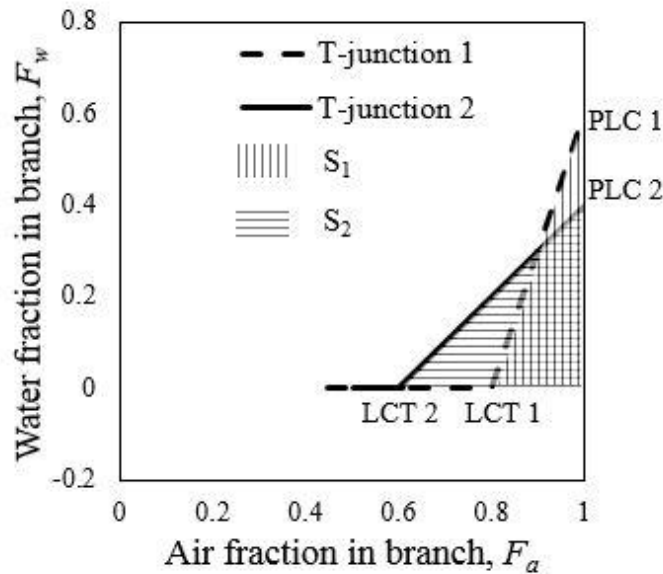


Figure 7. Illustration of dimensionless area of separation efficiency (*S*).

The dimensionless area of separation efficiency versus velocity ratio calculated from Wren [3], Saieed [1] and the present simulation data is shown in Figure 8. It became immediately apparent that when the velocity ratio increases, the performance of T-junction as separator decreases proportionally (the smaller the area, the better the performance). In other words, the performance of T-junction is directly proportional to the liquid superficial velocity and inversely proportional to the gas superficial velocity. This result is consistent with overall experimental data [25, 26] reported in the literature in the past 20 years. The generally accepted wisdom is that increasing liquid superficial

velocity leads to less liquid carryover because higher momentum causes liquid to go straight into the run arm. A period of non-monotonicity of  $S$  was detected in-between velocity ratio from 9.2 to 12.9, a phenomenon yet to be investigated further. It is suspected that this is the range where the gas has gained a good amount of momentum comparable to liquid. Using the standard error of estimate for  $S$ , there were slight differences between simulation and experiment, which are 0.8 % for Wren's data and 0.6 % for Saieed's data.

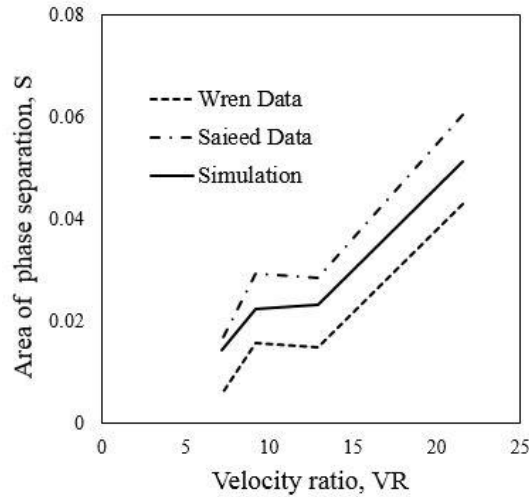


Figure 8. Dimensionless area of separation efficiency ( $S$ ) calculated from Wren [3], Saieed [1] and simulation data.

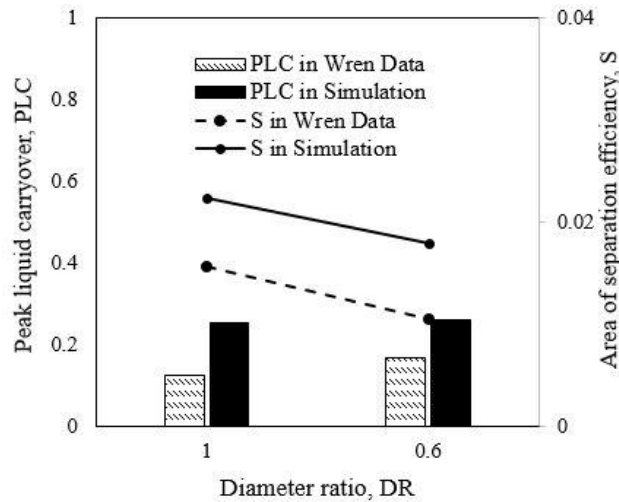


Figure 9. Peak liquid carryover ( $PLC$ ) and dimensionless area of separation efficiency ( $S$ ) in different  $DR$  from Wren [3] and simulation.

Figure 9 illustrates an outlier case to demonstrate the importance of including the dimensionless area when evaluating experimental data. Figure 9 showed  $PLC$  in reduced T-junction is higher than  $PLC$  in regular T-junction, which means regular T-junction performed better than reduced T-junction. This was in contradiction to the conclusion from Zetzman [27], Griston and Choi [28], Shoham [2, 29] and Azzopardi [30], which agreed that reduced diameter ratio T-junction delivered better phase separation. Meanwhile, a downward trend of  $S$  proved less liquid carryover in reduced T-junction. This can be concluded that using only  $PLC$  was not sufficient to evaluate phase separation

efficiency. In this case, the dimensionless area of separation efficiency should be counted as an additional evaluating parameters to compare separation performance. From this analysis, together with *PLC* and *LCT*, the dimensionless area of separation efficiency should be utilized in future research on T-junction to have a holistic evaluation.

## CONCLUSIONS

The CFD and 3D geometry model was carried out with the objective of simulating two-phase slug flow in T-junction and investigating the influence of diameter ratio and superficial velocities of air and water. Based on the results, conclusions could be drawn:

- The CFD model was able to reliably simulate the split of air-water flow in different geometry of T-junctions and also air and water superficial velocities. Standard estimate of error is 5.29% and 4.43% compared with experimental data of Wren [22] and Saieed [1]. Validated models gave reasonable accuracy, which can be used to predict phase separation efficiency in T-junction.
- Diameter ratio and superficial velocities of air and water have a great influence on phase separation efficiency. Reduced T-junction delivers less liquid carryover compared to regular T-junction. In slug flow regime, either decreasing air velocity or increasing water velocity can improve T-junction's performance.
- In addition to liquid carryover threshold (*LCT*) and peak liquid carryover (*PLC*), the dimensionless area of separation efficiency (*S*) was presented as a good parameter to measure and optimize T-junction. From this new concept, it is observed that for best phase separation, a T-junction must have low area of separation efficiency. Numerical results shows that area of phase separation is in a directly relationship with velocity ratio (*VR*).
- The results affirm model's authenticity and robustness and suggest the use of VOF methods in the study of two-phase flow in T-junction. A wider range of geometry and flow regime should be studied further using new proposed criteria to improve the phase separation efficiency.

## NOMENCLATURE

<i>A</i>	cross-sectional area	$m^2$
<i>C<sub>D</sub></i>	drag force coefficient	
<i>d</i>	pipe diameter	$m$
<i>f</i>	drag force	$Nm^{-3}$
<i>F</i>	mass flow rate ratio	
<i>g</i>	gravitational acceleration	$ms^{-2}$
<i>G</i>	gas mass flux	$kgm^{-2}s^{-1}$
<i>G<sub>k</sub></i>	generation of turbulent kinetic energy	
<i>I</i>	unit tensor	
<i>k</i>	turbulent kinetic energy	$m^2s^{-2}$
<i>L</i>	liquid mass flux	$kgm^{-2}s^{-1}$
<i>LCT</i>	liquid carryover threshold	
<i>m</i>	mass flow rate	$kg s^{-1}$
<i>P</i>	mixture pressure of 2 phases	$Pa$
<i>PLC</i>	peak liquid carryover	
<i>R</i>	body force (between 2 phases)	$N$

$R_e$	relative Reynolds number	
$S$	area of liquid carryover	
$SEE$	standard error of the estimate	
Greek letters		
$\alpha$	volume fraction	
$\varepsilon$	turbulent dissipation rate	$\text{m}^2\text{s}^{-3}$
$\mu$	dynamic viscosity	$\text{kgm}^{-2}\text{s}^{-1}$
$\mu_t$	turbulent viscosity	$\text{kgm}^{-2}\text{s}^{-1}$
$\sigma$	surface tension coefficient	$\text{Nm}^{-1}$
$\rho$	density	$\text{kgm}^{-3}$
$\tau$	stress strain tensor	
$\nu$	kinematic viscosity	$\text{m}^2\text{s}^{-1}$
$v$	velocity	$\text{ms}^{-1}$
$v_s$	superficial velocity	$\text{ms}^{-1}$
Subscripts		
$1,2,3$	main, run, branch arms	
$a$	air	
$g$	gas phase	
$i$	g or l	
$l$	liquid phase	
$m$	two-phase mixture	
$w$	water	

---

## ACKNOWLEDGEMENTS

The authors would like to acknowledge the funding by the Ministry of Higher Education through FRGS 0153AB-L03 and PETRONAS through YUTP Fundamental Research Grant 0153AA-E03.

## REFERENCES

- [1] Saieed, A., Two-phase separation in a T-junction, MSc Thesis, Universiti Teknologi PETRONAS, 2017.
- [2] Shoham, O., Brill, J.P., Taitel, Y., Two-phase flow splitting in a tee junction-experiment and modelling. *Chemical Engineering Science* 1987, 42, 2667–2676.
- [3] Wren, E., Geometric effects in phase split at a large diameter T-junction, Doctoral Thesis, University of Nottingham, 2001.
- [4] Baker, G., Clark, W.W., Azzopardi, B.J., Wilson, J.A., Controlling the phase separation of gas–liquid flows at horizontal T-junctions. *AIChE J.* 2007, 53, 1908–1915.
- [5] He, K., Wang, S., Zhang, L.-Z., Transient split features of slug flow at an impacting micro-T-junction: A numerical study. *International Journal of Heat and Mass Transfer* 2017, 112, 318–332.
- [6] Taitel, Y., Dukler, A.E., A model for predicting flow regime transitions in horizontal and near horizontal gas-liquid flow. *AIChE Journal* (Vol. 22, No. 1) 1976, 47.

- [7] Liu, Y., Li, W.Z., Numerical simulation on two-phase bubbly flow split in a branching T-junction. *Int. J. Air-Cond. Ref.* 2011, 19, 253–262.
- [8] Lu, P., Zhao, L., Deng, S., Zhang, J., et al., Simulation of two-phase refrigerant separation in horizontal T-junction. *Applied Thermal Engineering* 2018, 134, 333–340.
- [9] Lun, I., Calay, R.K., Holdo, A.E., Modelling two-phase flows using CFD. *Applied Energy* 1996, 53, 299–314.
- [10] Cook, M., Behnia, M., Bubble motion during inclined intermittent flow. *International Journal of Heat and Fluid Flow* 2001, 22, 543–551.
- [11] Lörstad, D., Fuchs, L., High-order surface tension VOF-model for 3D bubble flows with high density ratio. *Journal of Computational Physics* 2004, 200, 153–176.
- [12] Zhou, L., Liu, D., Ou, C., Simulation of Flow Transients in a Water Filling Pipe Containing Entrapped Air Pocket with VOF Model. *Engineering Applications of Computational Fluid Mechanics* 2011, 5, 127–140.
- [13] Taha, T., Cui, Z.F., CFD modelling of slug flow in vertical tubes. *Chemical Engineering Science* 2006, 61, 676–687.
- [14] Ujang, P.M., Lawrence, C.J., Hale, C.P., Hewitt, G.F., Slug initiation and evolution in two-phase horizontal flow. *International Journal of Multiphase Flow* 2006, 32, 527–552.
- [15] Ujang, P.M., Pan, L., Manfield, P.D., Lawrence, C.J., et al., Prediction of the translational velocity of liquid slugs in gas-liquid slug flow using computational fluid dynamics. *Multiphase Science and Technology* 2008, 20, 25–79.
- [16] Febres, M., Nieckele, A.O., Fonseca, R., Three-dimensional unit slug in a horizontal pipeline, in: *7th International Conference on Multiphase Flow, Florida USA 2010*.
- [17] Ban, S., Numerical simulation of two-phase slug flow regime in horizontal pipe, MSc Thesis, Universiti Teknologi PETRONAS, 2017.
- [18] Saieed, A., Pao, W., Hewakandamby, B., Azzopardi, B.J., et al., Experimental investigation on the effect of diameter ratio on two-phase slug flow separation in a T-Junction. *Journal of Petroleum Science and Engineering* 2018, 170, 139–150.
- [19] Saieed, A., Sam, B., Pao, W., Hashim, F.M., Numerical investigation of side arm gas volume fraction in two phase T-junction. *Journal of Mechanical Engineering and Sciences* 2016, 10, 2311–2323.
- [20] Baker, O., Design of pipelines for the simultaneous flow of oil and gas, in: *Fall Meeting of the Petroleum Branch of AIME, Society of Petroleum Engineers, 1953*.
- [21] Rusdin, A., Computation of turbulent flow around a square block with standard and modified k- $\epsilon$  turbulence models. *International Journal of Automotive and Mechanical Engineering* 2017, 14, 3938–3953.
- [22] Halim Abd, M.A., Nik Mohd, N.A.R., Mohd Nasir, M.N., Dahalan, M.N., The Evaluation of k- $\epsilon$  and k- $\omega$  Turbulence Models in Modelling Flows and Performance of S-shaped Diffuser. *International Journal of Automotive and Mechanical Engineering* 2018, 15, 5161–5177.
- [23] Saieed, A., Pao, W., Hashim, F.M., Effect of T-junction diameter ratio on stratified-wavy flow separation. *Journal of Natural Gas Science and Engineering* 2018, 51, 223–232.
- [24] Saieed, A., Pao, W., Ali, H.M., Prediction of phase separation in a T-Junction. *Experimental Thermal and Fluid Science* 2018, 97, 160–179.

- [25] Das, G., Das, P.K., Azzopardi, B.J., The split of stratified gas–liquid flow at a small diameter T-junction. *International Journal of Multiphase Flow* 2005, 31, 514–528.
- [26] Roberts, P.A., Azzopardi, B.J., Hibberd, S., The split of horizontal semi-annular flow at a large diameter T-junction. *International Journal of Multiphase Flow* 1995, 21, 455–466.
- [27] Zetzmann, K., Phasenseparation und Druckelufall in Zweiphasig Durchstroemten Vertikalen Rohrabzweigungen, Doctoral Thesis, University of Hannover, 1982.
- [28] Griston, S., Choi, J.H., Two-phase flow splitting at side-branching tees, in: *SPE Western Regional Meeting*, Society of Petroleum Engineers, 1998.
- [29] Shoham, O., Arirachakaran, S., Brill, J.P., Two-phase flow splitting in a horizontal reduced pipe tee. *Chemical Engineering Science* 1989, 44, 2388–2391.
- [30] Azzopardi, B.J., The Effect of Side Arm Diameter on Phase Split at T-Junctions, in: *SPE Annual Technical Conference and Exhibition*, Houston, Texas, USA 1999.